J Geophys (1986) 59:11–15

Journal of Geophysics

The effect of *SKS* scattering on models of the shear velocity-structure of the D" region

T. Lay and C.J. Young

Department of Geological Sciences, University of Michigan, Ann Arbor, Michigan 48109-1063, USA

Abstract. Several recent seismological models for the *P*- and *S*-wave velocity structure of the lowermost 300 km of the mantle (D" region) have proposed the existence of first-order discontinuities several hundred kilometers above the core-mantle boundary. Long-period transverse-component *S*-waves in the distance range 72°–95° provide the clearest evidence for a lower-mantle discontinuity. Arrivals between *SH* and *ScSH* in the range 72°–82°, and a double *S* arrival in the range 90°–95°, have been interpreted as effects of a lower-mantle triplication produced by a 2.75% velocity increase 280 km above the core. However, it is well established that the D" layer has significant lateral heterogeneity and caution must be exercised when interpreting lower-mantle signals with radially symmetric structures. This paper explores the possibility that the tangential component complexity, which has previously been interpreted by a discontinuity model, is actually produced by *SKS* contamination. It is shown that *SKS* has the wrong timing and ray parameter to possibly account for the *SH* observations in all but a small portion (77°–80°) of the triplication range (72°–95°). Even when strong *SKS* arrivals are apparent on the radial *SV* components, *SKS* contamination of the transverse components is usually very minor in the previously modeled long-period data. The fact that *SKS* is typically nodal in that data set further supports the lower-mantle discontinuity model interpretations. These results do not preclude the existence of lateral variations in the discontinuity or within the D" layer beneath it, and do not eliminate the need for caution to avoid possible *SKS* contamination in future data analysis.

Key words: Lower-mantle velocity structure – S-wave triplication – *SKS* signals – D" region – Velocity heterogeneity

Introduction

It is well established that the *P*- and *S*-wave velocity gradients at the base of the mantle are anomalous, being lower than gradients in the mid-mantle, and also that the lowermost 300 km of the mantle (D" region) has significant lateral heterogeneity. However, despite numerous studies of *P*- and *S*-wave signals, there is no agreement on the detailed characteristics of the velocity structure in D" (Cormier, 1985). Several recent studies, typically utilizing synthetic waveform modeling and careful analysis of large, high-quality data sets, are providing significant advances in our understanding of D" velocity structure. This is an exciting field of research, because accurate seismic models are critical for resolving the questions of compositional stratification of D" and the existence of any thermal boundary layer above the core-mantle boundary. These are important issues for models of the dynamic, petrological, and thermal evolution of the Earth.

Most seismological studies of the D" region have attempted to determine radially symmetric velocity models that satisfy either global travel time or diffracted *P*- and *S*-wave data sets (e.g. Doornbos and Mondt, 1979; Mula and Müller, 1980; Dziewonski and Anderson, 1981). These usually have resulted in velocity models with smooth negative or slightly positive velocity gradients throughout D". Generally, such studies incorporate significant horizontal averaging, reducing their sensitivity to fine details of the velocity structure. Also, given the abundant evidence for lateral heterogeneity of D", it is not clear whether the resulting models are even adequate "average" structures on which to base interpretations of the thermal structure of the region. Body-wave modeling studies that selectively sample separate regions of the D" layer promise to provide more detailed local velocity structures and hence better control on lateral variations. In most cases, it appears that the scale lengths of predominant lateral variations in D" are comparable to those in the upper mantle (Ruff and Lettvin, 1984; Lay and Helmberger, 1983a). By this we mean that when analyzing long-period bodywaves, regions with 1,000-km dimensions in D" have sufficiently stable behavior to allow determination of reliable local structures, as has also proved true in the more variable upper mantle (e.g. Grand and Helmberger, 1984; Walck, 1985).

Several recent detailed studies of *P* waveforms that sample isolated areas in the D" layer have indicated substantial fine velocity structure within D", as well as lateral variations in that fine structure (e.g. Ruff and Helmberger, 1982; Ruff and Lettvin, 1984; Wright and Lyons, 1981). In a recent *P* slowness study using a temporary network in Australia that recorded *P*-waves bottoming beneath southeast Asia, Wright et al. (1985) argue for the presence of a sharp increase in *P* velocity of 2.5%–3.0% about 160 km above the core-mantle boundary. It must be emphasized that all studies of short-period *P*-waves traversing the D" region are complicated by the scattering of the signals that occurs all along their paths, as well as by the intrinsically high *P* velocities in the lower mantle which inhibit isolation of discrete triplication branches, even in short-period data.

Offprint requests to: Thorne Lay

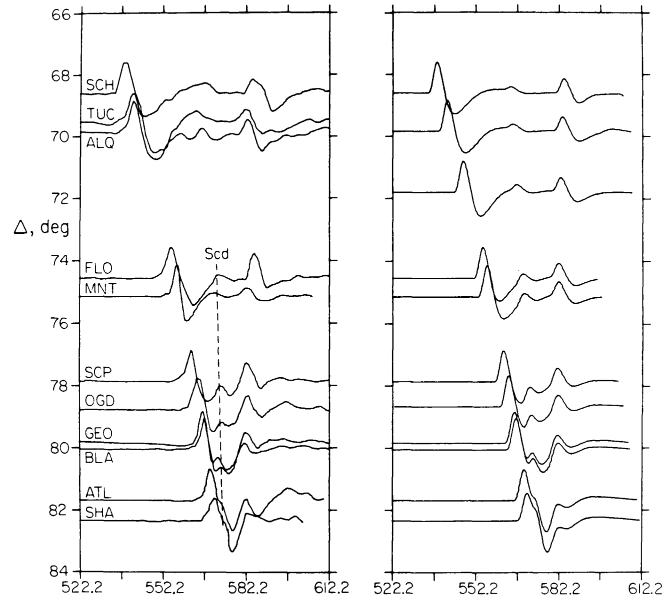

Fig. 1. Profiles of long-period tangential component data (*left*) and synthetics (*right*) for a deep-focus (583 km) earthquake in the Sea of Okhotsk. The stations are WWSSN and Canadian stations in North America. The first arrival in each trace is direct *S* and the arrival around 580 s is *ScS*. Note the arrival ahead of *ScS* which interferes with the downswing of *S*. This arrival, S_{cd}, is produced in the synthetics by the triplication resulting from the lower-mantle discontinuity in model SLHO (Fig. 2)

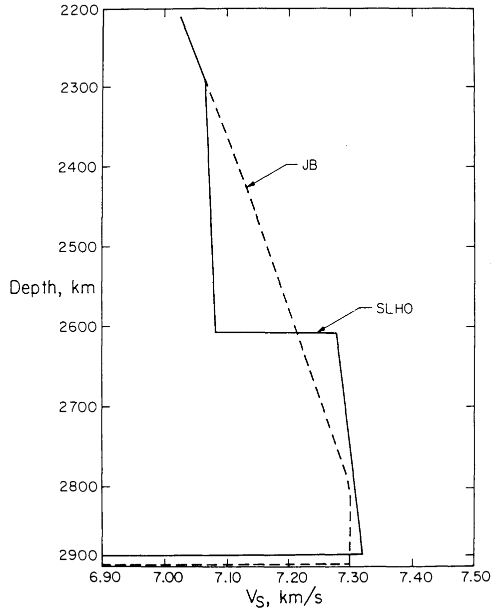

Fig. 2. Shear-velocity profiles in the D" region for the JB model and model SLHO of Lay and Helmberger (1983a), which was derived for paths bottoming beneath Alaska. SLHO has a 2.75% velocity increase 270 km above the core. Both models are identical above 2,200 km depth

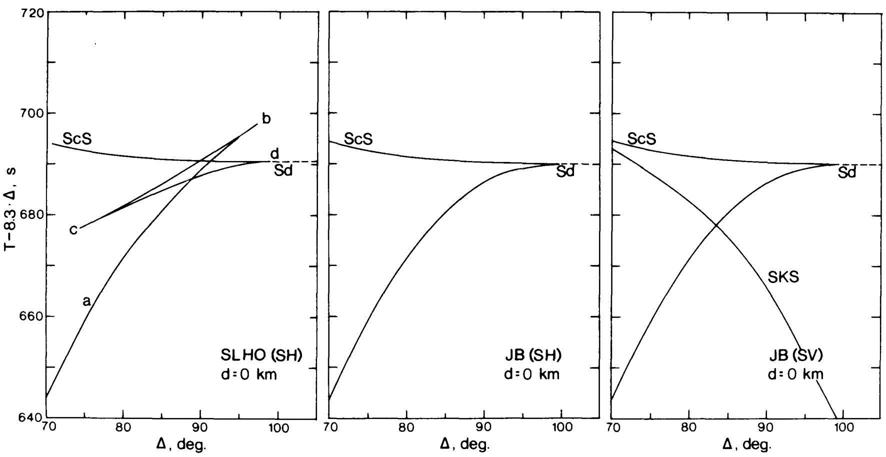

Fig. 3. Surface-focus travel-time curves for lower-mantle *S*-wave arrivals. The SLHO curve shows the triplication expected for a lower-mantle *S*-wave discontinuity compared with the *SH* travel-time curve for the JB model. The *SV* travel-time curve is for the JB model, and illustrates that *SKS* does arrive between *SV* and *ScSV* in the range 75°–85°, but with a much different $dT/d\Delta$ than the triplication arrivals in SLHO. *SKS* clearly cannot produce the interference seen near 95° where S_{ab} and S_{cd} spread apart beyond the crossover distance

Lay and Helmberger (1983a) utilized the fact that the *S*-wave velocities in D" are significantly lower than the *P* velocities in detecting a precursor to *ScSH* that reflects from a lower-mantle velocity discontinuity. Figure 1 shows an example of this arrival, which can be directly observed in rotated *SH* data profiles. This profile is for a 583-km-deep Sea of Okhotsk event recorded at North American stations spanning a narrow azimuth range from the source. The *S* and *ScS* arrivals are clear, as is the systematic arrival labelled *Scd*, which precedes *ScS* by about 10 s. This arrival produces a distinctive distance-varying interference pattern in the range 74°–80°. Observations of this arrival for numerous events with different source depths and distances led to the interpretation that the arrival results from a triplication produced by an abrupt 2.5%–3% shear-velocity increase above the core-mantle boundary. The model obtained for this particular path, SLHO, is shown in Fig. 2, along with a reference JB model, and synthetics for model SLHO are compared with the data in Fig. 1. The timing, amplitude, and interference effects of *Scd* are accurately predicted over the entire range.

Figure 3 shows an *SH* travel-time curve for the SLHO model indicating the timing of the *Scd* branch. As one would expect, the observed long-period *SH* signals in the distance range 82°–88° are generally quite simple, since all the triplication and *ScS* phases arrive within the instrument upswing. However, beyond 89° the triplication opens up again and two arrivals should be apparent. Lay and Helmberger (1983a) showed that this is in fact observed in the data, with the waveforms being modeled-well by SLHO.

However, as demonstrated by Schlittenhardt et al. (1985), synthetics for model SLHO do not closely match all observations in the range 95°–110°.

By analyzing numerous events in a given source region recorded by the same receiver array it is possible to empirically establish receiver structure effects, to determine the stability of the *Scd* arrival, and to develop an appropriate local D" structure for that particular path. Lay and Helmberger (1983a) did this for three D" samples (beneath Alaska, northern Eurasia, and the Caribbean) and in all cases, data throughout the range 70°–95° show waveform complexity that is well predicted by a discontinuity model. Variations of 50 km in the depth of the discontinuity were detected between the three regions sampled. However, the size of the velocity increase did not vary. The general consistency of the models for such different patches of D" suggests the possibility that the discontinuity is a global feature, embedded within the laterally varying D" structure, but much further data analysis is needed to test this hypothesis.

The proposal that there is a deep mantle velocity discontinuity has stimulated several additional studies of D". Cormier (1985) suggested that in some cases the *Scd* arrivals in Fig. 1 are the result of *SKS* contamination of the transverse components. This presumably would be the result of off-great-circle rotation of the *S*-polarization angle produced by near-receiver heterogeneity or by some complex distribution of heterogeneity in D". Schlittenhardt et al. (1985) argue that diffracted *S* and *P* profiles do not clearly show the expected post-critical refraction along the discontinuity and feel that the *ScS* precursor is due to some other phenomenon. Schlittenhardt (1983) calculated short-period *P*-wave synthetics for a D" model, with a 2.7% *P*-wave velocity discontinuity, and concluded that such a structure is not consistent with some *P*-wave observations. In this paper we explore the question of whether *SKS* contamination affects the data set initially utilized to detect the *Scd* arrival.

Analysis of *SKS* contamination

Figure 3 shows *SH* travel-time curves for the SLHO and JB models along with an *SV* travel-time curve for the JB model. *SKS* arrives between *SV* and *ScSV* in the distance range 80°–85°, which makes it difficult to use *SV* signals to model the D" region (Lay and Helmberger, 1983a, b). There is clearly a several degree range in which *SKS* arrives at the same time as the *Scd* branch. Figure 4 shows the longperiod waveform effects produced by *SKS* in the precrossover triplication range, for the two events analyzed by Lay and Helmberger (1983a, b) that have the strongest *SV* arrivals. In the range 78°–80° the *SKS* arrival peaks close in time to the arrival between *S* and *ScS* on the transverse components. It is plausible that given the relatively strong *SKS* arrivals, some contamination of the transverse components could occur, as suggested by Cormier (1985). Note, however, that this contamination must be systematic to produce the apparent moveout of the *Scd* arrival, and it must change in nature from station to station.

This possibility was explored further by computing *SV* and *SH* synthetic wavetrains for the smooth PREM model (Dziewonski and Anderson, 1981), which were then rotated onto incorrect back azimuths, allowing *SKS* to 'leak over' onto the '*SH*' in a procedure similar to that in Cormier (1985). Figure 5 shows a few results of this simulation, with

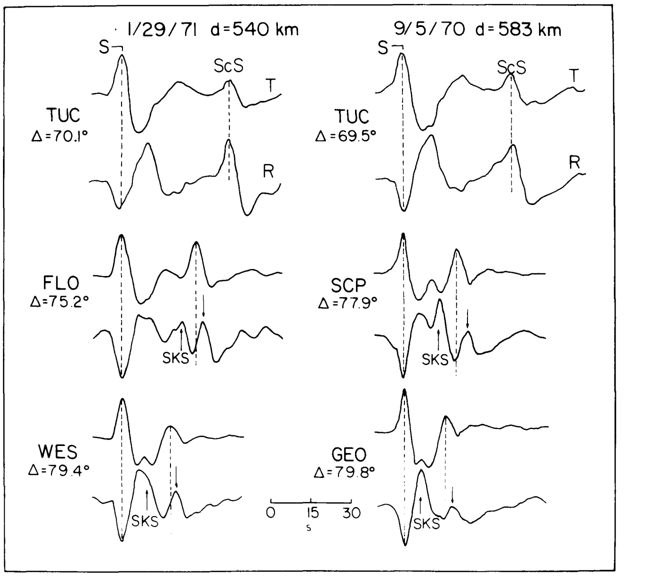

Fig. 4. Comparison of tangential (*T*) and radial (*R*) components of two deep-focus Sea of Okhotsk events recorded in North America. The *SH* and *SV* peak amplitudes arrive at the same time at all distances. The peak of the *SKS* arrivals on the radial components (arrows) are shown

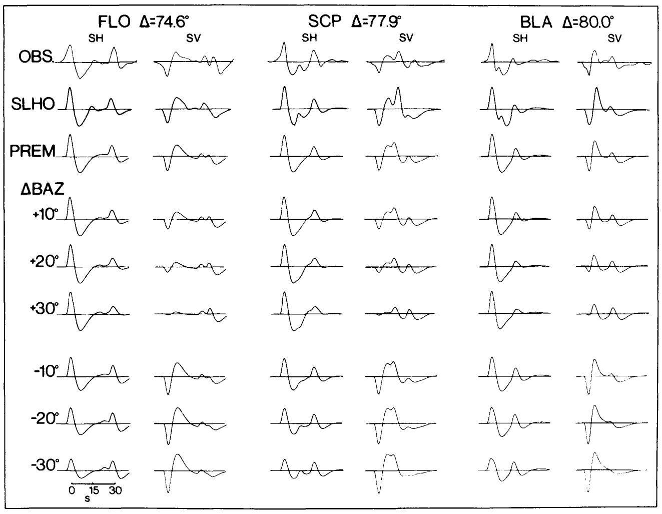

Fig. 5. Comparison of observed *SH* and *SV* waveforms for the Sea of Okhotsk event of 9/05/70 with synthetics for PREM and SLHO. Each *SH* and *SV* pair has true relative amplitude. The PREM synthetics are shown with incorrect back azimuth rotations in 10° increments to simulate *SKS* contamination of the *SH* component as advocated by Cormier (1985). Such contamination fails to reproduce the observed arrival between *S* and *ScS* at FLO and BLA, and mimics the SCP observation only with at least a 25° off-azimuth contamination that ruins the agreement with the *SV* waveform and the *SV*/*SH* amplitude ratio

observed waveforms from a Sea of Okhotsk event in the triplication range being compared with SLHO and PREM synthetics. For station FLO (74.6°), the small arrival between *S* and *ScS* apparent in the data and in the SLHO synthetics is never reproduced by the PREM models, regardless of the amount of *SKS* contamination. This is because *SKS* arrives only a few seconds ahead of *ScS*, well after the small arrival of the *SH* component, at this distance (see Fig. 3). For SCP (77.9°), it does prove possible to pro-

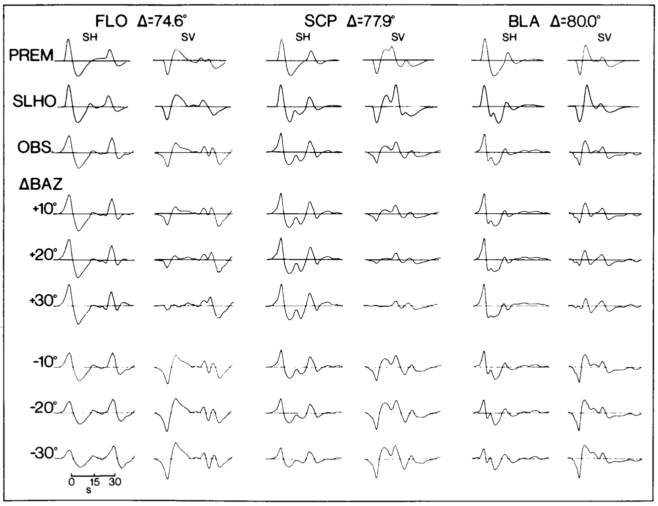

Fig. 6. A similar comparison to that in Fig. 5, but the data are shown with back azimuth rotations that deviate from the great circle by 10° increments. Note the stability of the arrival between *S* and *ScS* on the *SH* observations, even for back azimuth errors of 30°. This illustrates the predominantly *SH* character of this arrival, consistent with the model SLHO calculations

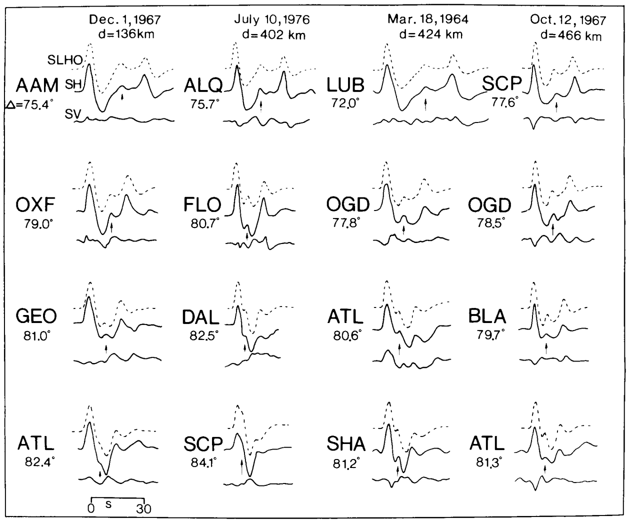

Fig. 7. Examples of *SH* and *SV* (radial) recordings with true relative amplitudes for Sea of Okhotsk events analyzed by Lay and Helmberger (1983a). The *dashed curves* show *SH* synthetics for model SLHO, which was constructed to produce the triplication arrival between *S* and *ScS* indicated by the *arrows*. Note that the very low amplitude radial components do not have strong *SKS* arrivals at these times.

duce an arrival between *S* and *ScS* at about the right time if a 25° off-azimuth *SKS* contamination is allowed. Note, however, that this results in a very clear degradation of the fit between the *SV* synthetic and the data, as well as an incorrect *SV*/*SH* amplitude ratio. For BLA (80°), the timing of *SKS* is again such that no back azimuth error in the PREM synthetics can produce the observed arrival between *S* and *ScS*, which is well matched by the SLHO discontinuity model. Similar calculations for stations at nearby ranges corroborate these findings.

Lay and Helmberger (1983a) show that in the range 72°–76° there are numerous picks of the *Scd* branch which

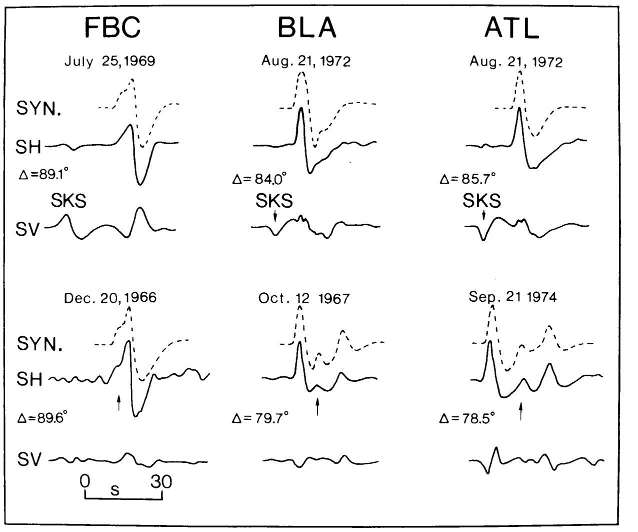

Fig. 8. Examples of stations recording *SH* and *SV* signals at distances where *SKS* is well ahead of the *S* arrival (see the travel-time curves in Fig. 3) along with closer observations at the same stations. Note that the typical *SKS* contamination apparent on the *SH* components is a very small fraction of the actual *SKS* amplitudes (the *SH* and *SV* components are on true relative scales). The *dashed curves* show *SH* synthetics for model SLHO. Note the agreement between the SLHO calculations and the observed data at these stations at all distances, including distances within the triplication range. This illustrates that receiver complexity is not responsible for the arrival between *S* and *ScS*, as well as showing that *SKS* cannot produce the waveform complexity beyond crossover distance (near 90°)

cannot be attributed to *SKS*, which arrives much to late. Thus, in this distance range the *Scd* observations clearly require a different explanation than *SKS* contamination. The possibility of receiver reverberations was ruled out in their study by individual station analysis.

Figure 6 is similar to Fig. 5 except that the *data* are shown rotated with back azimuths departing from the great circle. The arrival between *ScS* and *S* on the *SH* component does not vary significantly, even for large off-great-circle rotations. This stability testifies to the predominantly *SH* character of the arrival. The tests in Figs. 5 and 6 were conducted for the event with the strongest *SV* and *SKS* arrivals of all the events used by Lay and Helmberger (1983a). Figure 7 presents much more typical examples of *SH* and *SV* waveforms in the triplication range for several of their events. Each *SH* and *SV* pair is plotted with true relative amplitude. There are no strong *SKS* arrivals on the radial components at the time of the *Scd* arrivals (arrows), and the *SH* waveforms are modeled well by the SLHO synthetics. The observed *SV*/*SH* amplitude ratios are very consistent with the known *P*-wave first motion mechanisms of these events (Lay and Helmberger, 1983a). There is no reason to believe that the *S*-waves are so strongly contaminated by near-receiver structure that *all* of the *SV* signal ends up on the transverse components when the great-circle back azimuth is assumed in the rotation.

By examining observations beyond 84°, where *SKS* is an isolated first arrival (see Fig. 3), one can obtain a better estimate of how much *SKS* contamination actually does occur. Figure 8 shows examples of recordings at this distance as well as recordings at closer distances for the same stations. For these stations, rotation assuming the great-circle back azimuth leads to less than 10% contamination of the *SKS* signal on the *SH* component. These same stations show strong *Scd* arrivals within the triplication range, but these are not accompanied by *SKS* signals at least ten times as strong on the radial component. Indeed, the *SKS* arrivals are observed to be nodal, as predicted by the known focal mechanisms. It is also clear in Fig. 8 that the *SKS* signals cannot possibly account for the double *S* arrivals observed near 90° (see Figs. 16, 34, and 37 of Lay and Helmberger, 1983a), because *SKS* is well ahead of the *S* arrival at this distance. These arguments refute the possibility that the discontinuity models are invalid because of *SKS*. It is important to note that this conclusion is based on the long-period waveforms. Short-period waveforms (and occasionally long-period records from notorious stations like OXF) in our data set often show appreciable *SKS* contamination on the transverse component, partially due to the greater difficulties in accurately digitizing and rotating the short-period records. Thus, analysis of short-period or broadband *S*-waves must be performed very carefully, and optimally for events with nodal *SV* arrivals. Zhang and Lay (1984) analyzed data from an array of broadband stations for such events and still found tremendous receiver complexity effects that must also be accounted for.

Discussion

In this paper we have concentrated on establishing whether *SKS* contamination has led to a misinterpretation of lower-mantle shear-velocity structure by Lay and Helmberger (1983a). There appears to be very little evidence to support this possibility, as it could require a tremendous number of special circumstances to account for the consistency of the *SH* data and to explain away the lack of *SKS* signals on the radial components. Clearly the D" layer has lateral heterogeneity, and any radial model (even for a localized portion of the D" region) may be in error to some degree because it attributes scattered effects to a deterministic radial structure. However, the consistency of the observations for nearby stations and from event to event strongly indicates that such errors in the discontinuity models are minor. It has proved possible to determine reliable upper-mantle velocity structures for different tectonic regions despite 10% velocity heterogeneity, which probably greatly exceeds variations in D". There is no question that modeling the D" region is difficult, and data-intensive studies are the best way to reliably account for upper-mantle, source, and receiver effects. While all earth models are undoubtedly simplifications of the actual structure, if they are able to predict the detailed behavior of many observations it seems reasonable to believe they are valid, at least to first order.

Much additional analysis of lower-mantle *P*- and *S*-waves is certainly needed, particularly with regard to possible anisotropy and variations in fine scale features. This modeling must be performed with an open mind toward both possible stratification, general heterogeneity, and apparent or intrinsic anisotropy, as advocated by Cormier (1985), given the proximity of D" to the largest compositional and density discontinuity within the Earth.

Conclusions

A detailed analysis of *SV* and *SH* waveforms in the distance range 72°–95° has been performed with the intent of appraising the possibility that *SKS* contaminates the transverse components leading to incorrect D" velocity models. For the data which has previously been interpreted as evidence of a lower-mantle shear-velocity discontinuity, it is very unlikely that *SKS* has caused any systematic problem. The strongest argument for this is that in the majority of the data the *SKS* arrival is much smaller than the arrivals on the transverse component, consistent with the known radiation patterns. Furthermore, the timing of *SKS* is not the same as that of the triplication arrivals on the *SH* components except over a narrow in distance. Well-controlled experiments show that typically less than 10% of the *SKS* waveform contaminates long-period *SH* signals rotated assuming the great-circle back azimuth.

Acknowledgements. We thank V.F. Cormier and D. Helmberger for discussions on this analysis. Comments on the manuscript by the two reviewers and G. Müller are appreciated. C.J.Y. was partially supported by a University of Michigan Regent's Fellowship. This research was supported by the National Science Foundation under Grant NSF EAR 8407792.

References

Cormier, V.F.: Some problems with S, SKS, and ScS observations and implications for the structure of the base of the mantle and the outercore. J. Geophys. **57**, 14–22, 1985

Doornbos, D.J., Mondt, J.C.: P- and S-waves diffracted around the core and the velocity structure at the base of the mantle. Geophys. J. R. Astron. Soc. **57**, 381–395, 1979

Dziewonski, A.M., Anderson, D.L.: Preliminary reference earth model. Phys. Earth Planet. Int. **25**, 297–356, 1981

Grand, S., Helmberger, D.V.: Upper mantle shear structure of North America. Geophys. J. R. Astron. Soc. **76**, 399–438, 1984

Lay, T., Helmberger, D.V.: A lower mantle S-wave triplication and the shear velocity structure of D". Geophys. J. R. Astron. Soc. **75**, 799–838, 1983a

Lay, T., Helmberger, D.V.: The shear-wave velocity gradient at the base of the mantle. J. Geophys. Res. **88**, 8160–8170, 1983b

Mula, A.H., Müller, G.: Ray parameters of diffracted long period P- and S-waves and the velocities at the base of the mantle. Pageoph. **18**, 1272–1292, 1980

Ruff, L., Helmberger, D.V.: The structure of the lowermost mantle determined by short period P-wave amplitudes. Geophys. J. Astron. Soc. **68**, 91–119, 1982

Ruff, L., Lettvin, E.: Short period P-wave amplitudes and variability of the core shadow zone boundary. EOS **65**, 999, 1984

Schlittenhardt, J.: Investigation of the velocity structure of the lowermost mantle with short period PcP/P amplitude ratios (abstract). IASPEI Program and abstracts, XVIII General Assembly, IUGG, 259, 1983

Schlittenhardt, J., Schweitzer, J., Müller, G.: Evidence against a discontinuity at the top of D". Geophys. J. R. Astron. Soc. **81**, 295–306, 1985

Walck, M.: The upper mantle beneath the northeast Pacific rim: a comparison with the Gulf of California. Geophys. J. R. Astron. Soc. **81**, 243–275, 1985

Wright, C., Lyons, J.A.: Further evidence for radial velocity anomalies in the lower mantle. Pageoph. **119**, 137–162, 1981

Wright, C., Muirhead, K.J., Dixon, A.E.: The P-wave velocity structure near the base of the mantle. J. Geophys. Res. **90**, 623–634, 1985

Zhang, J., Lay, T.: Investigation of a lower mantle shear wave triplication using a broadband array. Geophys. Res. Lett. **6**, 620–623, 1984

Received July 16, 1985; Revised version October 4, 1985
Accepted October 15, 1985